Mn-doped II-VI quantum dots: artificial molecular magnets

J. Fernández-Rossier[*1] and **R. Aguado**[2]

[1] Departamento de Fìsica Aplicada, Universidad de Alicante, 03690 Spain
[2] Instituto de Ciencia de Materiales de Madrid, CSIC, 28049 Madrid,Spain

Received 1 May 2006, accepted 14 June
Published online 24 November 2006

Key words Quantum magnet, Quantum Dot, Diluted Magnetic Semiconductor
PACS 04A25

The notion of artifical atom relies on the capability to change the number of carriers one by one in semiconductor quantum dots, and the resulting changes in their electronic structure. Organic molecules with transition metal atoms that have a net magnetic moment and display hysteretic behaviour are known as single molecule magnets (SMM). The fabrication of CdTe quantum dots chemically doped with a controlled number of Mn atoms and with a number of carriers controlled either electrically or optically paves the way towards a new concept in nanomagnetism: the artificial single molecule magnet. Here we study the magnetic properties of a Mn-doped CdTe quantum dot for different charge states and show to what extent they behave like a single molecule magnet.

1 Introduction

One of the most studied single molecule magnets (SMM), Mn_{12}, is made of a cage of one hundred Carbon, Hydrogen and Oxygen atoms, surrounding a $Mn_{12}O_{12}$ cluster [1]. The oxydation state of the Mn atoms either $+3$ or $+4$ so that their spin is either (S=2) or (S=$3/2$). In the lowest energy configuration, the molecule has total spin $S = 10$ that results from the super-exchange interactions between the Mn spins [2]. The $S = 10$ manifold has 21 states that, due to the spin-orbit interaction, are split according to $E = -DS_z^2$, where S_z is the spin projection along a crystallographic axis z [2, 3]. Remarkably, the magnetization of a molecular crystal of Mn_{12} shows hysteresis, at temperatures larger than the inter-molecular coupling, reflecting that each individual molecule behaves as a magnet[3]. In marked contrast to mono-domain magnets, the hysteresis curve of a Mn_{12} crystal displays steps at well defined values of the applied field. These are associated to quantum tunneling events of the magnetic moment. Therefore, the magnetic moment of SMM behaves quantum mechanically [4].

As an extension of the concept of artificial atom [5], we propose the notion of artificial SMM: a II-VI semiconductor quantum dot, chemically doped with Mn atoms and electrically doped with carriers so that they form a collective spin that has meta-stable states (hysteresis) and steps in the magnetization. As a substituional impurity of the cation in the II-VI material [6], Mn is in a $2+$ oxydation state with spin $S = 5/2$. In our device there are a few Mn atoms, sufficiently apart as to make the antiferromagnetic exchange interaction between them completely negligible. The magnetic properties of the dot are given by the controlled presence of electrons and/or holes in the conduction and valence band quantum dot levels. Since both electrons and holes are exchanged coupled to the Mn spin [6], indirect exchange interactions couple the Mn spins to each other [7] in the dot. Even in the case of a dot doped with a single Mn atom, we show that the anisotropic spin interaction of the holes and the Mn [8, 9, 10, 11, 12, 13] results in SMM behaviour.

* Corresponding author: e-mail: jfrossier@ua.es, Phone: +00 999 999 999, Fax: +00 999 999 999

Most of the working principles of this proposal have been verified experimentally. On one side, the charge state of II-VI quantum dot can be prepared, with a single electron accuracy, both by electrical[14, 15, 16] and optical means [17, 18]. On the other side, several groups have reported the fabrication if II-VI quantum dots doped with Mn atoms, and the exchange coupling of electrons and holes to the Mn spins [19, 20, 21, 22, 23, 24]. More recently, the controlled fabrication of CdTe quantum dots doped with a single Mn atom [8, 9, 10], as well as the electrical control of the charge state of a single CdTe quantum dot doped with a single Mn atom [13] and a GaAs island doped with tens of Mn atoms [25] have been reported. Electrical control of the carrier density has been demonstrated in larger magnetic semiconductor structures, making it possible to alter reversibly properties of the material like the T_C [26, 27] and the coercive field [28] of these systems. Our proposal targets the achievement of this notion at the scale of a single electron and the single Mn atom limit.

Related theory work has focused on the electronic structure [7, 29, 30, 31, 32], optical response [11, 33, 34] and transport [12, 35] of Mn-doped quantum dots as a function of the number of confined carriers. It is now well established that, depending on the number of carriers present in the dot, the eigenstates of the Mn-fermion Hamiltonian are very different [7]. In previous work we have derived from numerical diagonalizations [12] the effective spin Hamiltonian for relevant low energy sector of a CdTe dot doped with a single Mn interacting with up to 3 carriers, either electrons or holes. Here we give a preliminary account of the magnetization curves of a single CdTe dot, doped with a Mn atom, as a function of the number of carriers. The results presented here permit to claim that Mn-doped quantum dots with extra holes behave like a nanomagnet, with hysteretic magnetization and steps of the magnetization at precise values of the applied field.

The rest of this paper is organized as follows. In section II we summarize the model Hamiltonian for a Mn-doped CdTe quantum dot and we review the properties of the eigenstates and eigenvalues of the Hamiltonian for a given charge state $\mathcal{Q} = \pm 1, \pm 2, \pm 3$. In section III the magnetization of the dot with $\mathcal{Q} = +1$ and a single Mn is calculated. We first show that the equilibrium magnetization is anisotropic, in contrast to the free Mn case, due to the interaction to the hole. Then we discuss how the magnetization behaves if the field is varied so that equilibrium can not be reached, which can be the standard situation provided the long spin relaxation time of this system.

2 Hamiltonian

We consider quantum dots with a typical size of 10 nanometers and several thousand atoms, beyond reach of present-day ab-initio calculations [31]. This justifies the use of the standard model Hamiltonian [6, 7, 11, 12, 32, 33, 34, 35] for diluted magnetic semiconductors that describes CB electrons and VB holes interacting with localized Mn spins ($\vec{M}_I$) via a local exchange interaction and their coupling to an external magnetic field, $\vec{B}$. The Mn spins interact also with each other via short range superexchange coupling. In general the Hamiltonian can not be solved exactly and in most instances mean field or some other approxiamations are used. Only in the limit of a few Mn atoms and a few electron and hole states considered in this paper it is possible to diagonalize the Hamiltonian numerically without approximations. The second quantization Hamiltonian of the isolated dot reads:

$$\mathcal{H}_{QD} = \sum_{\alpha,\alpha'} \left(\epsilon_\alpha(\vec{B})\delta_{\alpha,\alpha'} + \sum_I J_{\alpha,\alpha'}(I)\vec{M}_I \cdot \vec{S}_{\alpha,\alpha'}(\vec{R}_I) \right) f_\alpha^\dagger f_{\alpha'} + \sum_{I,J} J_{IJ}^{\mathrm{AF}} \vec{M}_I \cdot \vec{M}_J \qquad (1)$$

Here $f_\alpha^\dagger$ creates a band carrier in the α single particle state of the quantum dot, which can be either a valence band or a conduction band state. QD carriers occupy localized spin orbitals ϕ_α with energy ϵ_α which are described in the envelope function $\vec{k} \cdot \vec{p}$ approach [7, 11, 12, 36]. In the case of valence band holes the 6 band Kohn-Luttinger Hamiltonnian, including spin orbit interaction, is used as a starting point to build the quantum dot states [36]. The first term in the Hamiltonian describes non interacting carriers

in the dot and the second term describes the exchange coupling of the carriers and the Mn. We neglect interband exchange so that $J_{\alpha,\alpha'} = J_e$ ($J_{\alpha,\alpha'} = J_h$) if both α and α' belong to the conduction band states (valence band states). In contrast, we include exchange processes by which a carrier is scattered between two different levels of the dot that belong to the same band are included, although the level spacing considered here is much larger than the exchange interaction. The matrix elements of both valence and conduction band spin density, evaluated at the location of the Mn atoms, are given by $\vec{S}_{\alpha,\alpha'}(\vec{R}_I)$. They depend strongly on the orbital nature of the single particle level in question. In the case of conduction band we neglect spin orbit interactions so that $\vec{S}_{\alpha,\alpha'}$ is rotationally invariant [7]. In contrast, strong spin orbit interaction of the valence band makes the Mn-hole interaction strongly anisotropic [11, 36, 37, 38] and it varies between different dot levels. Following previous work [7, 11, 36] confinement is described by a hard wall cubic potential with $L_z < L_x \simeq L_y$. Although real dots are not cubic, this simple model [36] predicts properly that the lowest energy hole doublet has a strong heavy hole character, with spin quantized along the growth direction z whereas the next single particle doublet is mainly light hole with spin quantized in the xy plane.

As discussed in our previous work [12], in the case of $\mathcal{Q} = \pm 1$ and $\mathcal{Q} = \pm 3$ the low energy properties of $\mathcal{H}_{QD}$ are described by

$$\mathcal{H}_{eff} = \sum_{I,a=x,y,z} j_I^a \tau^a M_I^a + \sum_{a=x,y,z} \mu_B B_a \left(g M_I^a + g_a(\mathcal{Q})\tau^a\right) + \sum_{I,J} J_{IJ}^{\mathrm{AF}} \vec{M}_I \cdot \vec{M}_J \qquad (2)$$

where τ^a are the Pauli matrices operating on the isospin space defined by the lowest energy single particle doublet. In the case $\mathcal{Q} = -1, -3$ we have $j^x = j^y = j^z$. In the case $\mathcal{Q} = +1$ we have $j^x = j^y = 0$ in the absence of light-heavy hole mixing ($L_x = L_y$). In the case $\mathcal{Q} = +3$ we have $j^z < j^x = j^y$.

Hereafter we only consider dots with one Mn atom. Therefore, Mn-Mn superexchange interaction is irrelevant. The coupling of Mn to conduction band electrons is spin rotational invariant, so that the ground state manifold for $\mathcal{Q} = -1, 3$ are given by the 7 states with $S = 3$ and $S_z = \pm 3, \pm 2, \pm 1, 0$. In contrast, the Mn-hole coupling is very anisotropic. In a dot with $\mathcal{Q} = +1$ and $L_x = L_y$ spin-flip Mn-hole interactions are strictly forbidden. The resulting Ising coupling between the Mn and the hole yields a spectrum with 6 doublets. Their wave functions are given by $|M^z, S_h^z\rangle$ with and the eigen-values $E_{M^z,S^z} = |j_z| M^z \times S^z$, where $j^z = J_h |\psi(\vec{R}_{Mn})|^2$. The lowest energy doublet corresponds to the Mn spin maximally polarized against the heavy hole spin, which lies along the growth direction, z. The addition of a second holes fills the heavy hole doublet. The low energy sector has 6 states, spin splitted according the absolute value of the third component the Mn spin, the lowest energy is given by the $M_z = \pm 1/2$ doublet. This splitting comes from inter-level exchange coupling, which are of order Δ^2/δ [7]. . The addition of a third hole into the same dot leaves a doubly occupied heavy hole doublet and a singly occupied light hole interacting with the Mn. The different spin-orbital properties of the light hole result in an exchange coupling to the Mn which is in between the isotropic Heisenberg coupling of $\mathcal{Q} = -1$ and the Ising coupling of $\mathcal{Q} = +1$. The picture emerging from these results is the following: the low energy states of the Mn-fermion complex are spin-split at zero applied field. The spin splitting Δ is much larger for open shell configurations than for closed shell configurations. The symmetry properties of the lowest energy states are different for electrons, heavy holes and light holes.

3 Magnetic response

Now we address the magnetic properties of the single Mn doped CdTe dot although the results also scale for larger N. We calculate the many-body spectrum of the dot as a function of an external magnetic field. Since the single particle level spacing is much larger than the cyclotron frequency, it is not a bad approximation

to neglect the orbital magnetism. The magnetization is given by :

$$\langle \vec{\mathcal{M}} \rangle = \sum_N \langle N | \rho \left(\sum_I g \mu_B \vec{M}_I + g_f \mu_B \vec{S}_f \right) | N \rangle = \langle \vec{\mathcal{M}} \rangle_{Mn} + \langle \vec{\mathcal{M}} \rangle_f \tag{3}$$

where ρ is the quantum dot density matrix andg_f denotes the gyromagnetic factor of electrons and holes.

3.1 Equilibrium Results

In a first stage we assume that the density matrix of the quantum dot is that of thermal equilibrium. We consider the case of a dot with $\mathcal{Q} = +1$. At zero magnetic field the eigenstates with opposite magnetization are degenerate so that their populations are identical and the average magnetization vanishes. This is a consequence of the ergodic approximation, that assigns equal weight to the states of identical energy, and to time reversal symmetry. Application of a magnetic along the easy direction z splits the energy levels without mixing them, since $B_z M^z + B_z S^z$ conmutes with the Hamiltonian. The resulting energy diagram is shown in figure 1, lower left panel, and features numerous level crossings, reflecting the absence of transverse interactions. The magnetic field breaks the degeneracy of all the doublets, including the lowest energy one.

At temperatures smaller than the Zeeman splitting only the ground state is occupied, resulting in a net magnetization $\langle \vec{M} \rangle$, shown in the upper panel of figure 1. We show the Mn magnetization only because is dominant and simplifies the discussion. In that figure we show the magnetization of the dot with $\mathcal{Q} = 0$, which is the standard Brillouin function for $S = 5/2$. It is apparent that the $\mathcal{Q} = 0$ magnetization is softer than the $\mathcal{Q} = +1$ magnetization curve when the field is applied along the z direction, due to the exchange splitting of the levels with smaller $|M_z|$. This result is in agreement with previous work for exciton polarons [39] In contrast, the magnetization curve when the field is applied in the x direction, transverse to the easy axis of the dot, is much smaller than the free case. This is due to the competition between exchange interactions, that favor the alignment of the Mn along the z axis and the magnetic field. The difference is also seen in the energy spectrum, in the lower right panel. Hence, the presence of a heavy hole in the dot would result in a strong magnetic anisotropy in the equilibrium magnetization

3.2 Non-equilibrium results

The relaxation of the Mn-fermion spin towards equilibrium comes from the release of energy and angular momentum to their environment[40]. Since this process can be very slow, we need to consider a non-equilibrium density matrix. The relaxation time $T_1^{\mathcal{Q}=0}$ for Mn spins in very dilute CdMnTe can be as long as 10^{-3} s[41]. In the case of a $N = \mathcal{Q} = +1$ dot, the transitions between the two members of the ground state, $|\pm 5/2, \mp 1/2\rangle$ require a energy conserving perturbation that changes the Mn spin by $5\hbar$ and the hole angular momentum by $3\hbar$ in the opposite direction. Such a process is highly forbidden and his lifetime $T_1^{\mathcal{Q}=+1}$ will be definitely larger than $T_1^{\mathcal{Q}=0}$. Therefore, if the applied field is varied more rapidly than $T_1^{\mathcal{Q}=+1}$ we are not entitled to use the equilibrium density matrix.

Now we revisit the results of the previous subsection. We assume that the Ising Hamiltonian is perturbed by very weak additional terms that will only be effective close to degeneracy points in the energy diagram of figure 2. They read:

$$\mathcal{V} = a \left((M^x)^4 + (M^y)^4 \right) + \sum_i \mathcal{J}_i \vec{M} \cdot \vec{I}_i + \epsilon \left(M^x \tau^x + M^y \tau^y \right) \tag{4}$$

The so called cubic field term is the lowest order magnetic anisotropy term allowed by the crystal symmetry [41] and makes it possible to flip the Mn spin by 4 units. The second term comes from the hyperfine coupling of the Mn d electrons to the nuclear spins $\vec{I}$ [41]. It can flip the Mn spin by one unit. The last term arises from light-hole heavy-hole mixing and permits the transition of the hole via exchange of

one unit of angular momentum with the Mn. Other terms like dipolar coupling to the nuclear spins, of phonon-mediated hole spin relaxation might be involved as well.

Our starting point is a the dot under the influence of a large magnetic field along the positive z axis at low temperatures so that we assume that the dot is in the ground state, $|+\frac{5}{2},\downarrow\rangle$. Now the applied field is reduced down to zero, so that the state $E(+\frac{5}{2},\downarrow)$ becomes degenerate to $E(-\frac{5}{2},\uparrow)$. None of the terms in (4) can induce the transition from the former to the latter. It would take the combined action of several of them to achieve the spin-relaxing transition, which is thereby very slow. Hence, it would be possible to ramp the field through that degneracy point without spin relaxation. In that case the magnetization at zero field would be finite. The field could be reversed down to the crossing point of the state $|+\frac{5}{2},\downarrow\rangle$ with the state $|-\frac{3}{2},\uparrow\rangle$. The cubic field term can flip the Mn spin, and it would take further spin relaxation of the hole to achieve that transition. The quantum transition could take place here, or it could happen at larger fields, where the initial state is brought in to coincidence with $|-\frac{3}{2},\downarrow\rangle$, which is accesible via the cubic field term only. Further increase of the field towards negative value would bring into resonance the $|-\frac{3}{2},\sigma_h\rangle$ levels with the $|-\frac{5}{2},\uparrow\rangle$, completing the magnetization reversal process. In any case the magnetization displays remanence, hysteresis and abrupt steps as we show in the lower panel of figure 2. These are very similar to those observed in single molecule magnets [2, 3, 4]. This phenomenology is the consequence of the blocking of magnetization relaxation processes except at well defined values of the applied field that put levels with different M_z in resonance.

4 Discussion and Conclusions

Artifical atoms mimic the properties of natural atoms at much larger (smaller) length (energy) scale. From that point of view, artificial SMM is a hybrid device. The magnetic moment of both artificial and standard SMM comes from the Mn atoms. What makes them different is the glue that determines the total magnetic moment of the SMM. The properties of Mn_{12} come from the chemical bonding between the Mn and the oxygen atoms in the central core of the molecule. In the case of artificial SMM, the glue electrons are delocalized in a much larger length scale.

Measurement of the quantum features in the magnetization of molecular magnets is greatly simplified due to the homogeneity of the single molecule magnets in macroscopic molecular crystals. In the case of artificial molecular magnets, these specific values of the field that result in steps in the magnetization depend on the Mn-hole exchange coupling constant, which depends both on the dot size and on the Mn location inside the dot. Therefore, the measurement of magnetization over an ensemble of dots would yield results different from those shown in figure 3.

The measurement of the effect predicted here would require either the fabrication of extremely monodisperse dots, using for instance colloidal techniques [42], or the measurement of the magnetization of a single device. The second possibility is starting to be explored experimentally in the case of Mn_{12} molecules [43, 44]. We have studied recently the theory of a similar device in which Mn_{12} is replaced by a single Mn-doped CdTe quantum dot . We have shown that the magnetic state of the Mn determines the conductance of the dot. This opens the door for the measurement of $M(B)$ in a single dot. An additional experimental route could come from spin-selective optical measurements of a single dot. In summary, we claim that a Mn-doped CdTe quantum dot charged with a single heavy hole will have exotic magnetic properties that correspond to those of single molecule magnets. A single electron transistor with a single-Mn doped CdTe quantum dot would behave like an artificial single molecule magnet.

Acknowledgements This work has been financially supported by MEC-Spain (Grants FIS200402356, MAT2005-07369-C03-03, and the Ramon y Cajal Program) and by Generalitat Valenciana (GV05-152). This work has been partly funded by FEDER funds.

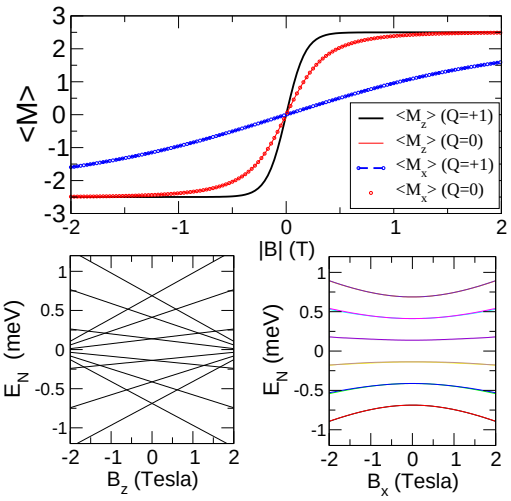

Fig. 1 Upper panel: equilibrium magnetization for dot with $\mathcal{Q} = 0$ and $\mathcal{Q} = +1$ with the field applied both along the growth axis and in-plane. Lower Panel: Energy spectrum for the dot as a function of B_z (left) and B_x (right).

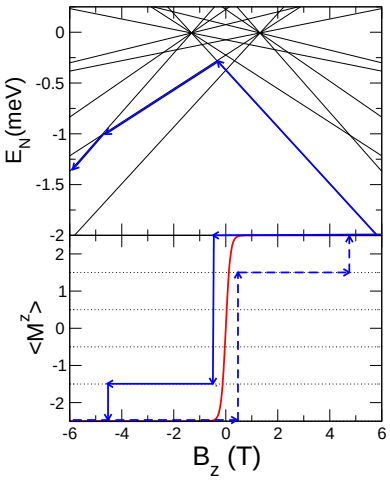

Fig. 2 Upper panel: detail of the Mn-hole spectrum and a possible non-ergodic evolution of the density matrix. Lower panel: non-ergodic magnetization of the system.

References

[1] T. Lis, Acta Crystallogr. Sect. B **36**, 2042 (1980)
[2] D. Gatteschi and. R. Sessoli, Angew. Chem. **42**, 268 (2003)
[3] J. R. Friedman *et al.*, Phys. Rev. Lett. **76**, 3830 (1996)
[4] J. Tejada, E. M. Chudnovsky, *Macroscopic Quantum Tunneling of the Magnetic Moment*, Cambridge University Press, Cambridge (1998)
[5] P. Hawrylak, Phys. Rev. Lett. **71**, 3347 (1993) L.P. Kouwenhoven *et al.* Science **278**,1788 (1997)
[6] J. K. Furdyna, J. Appl. Phys **64** R29 (1988).
[7] J. Fernández-Rossier and L. Brey, Phys. Rev. Lett. **93** 117201 (2004)
[8] L. Besombes, Y. Lger, L. Maingault, D. Ferrand, H. Mariette and J. Cibert Phys. Rev. Lett. **93**, 207403 (2004)
[9] L. Besombes, Y. Leger, L. Maingault, D. Ferrand, H. Mariette, and J. Cibert Phys. Rev. B. **71**, 161307 (2005)
[10] Y. Léger L. Besombes, L. Maingault, D. Ferrand, and H. Mariette, Phys. Rev. Lett. **95**,047403 (2005)
[11] J. Fernández-Rossier, Phys. Rev. B.**73**, 045301 (2006)
[12] J. Fernández-Rossier, R. Aguado, cond-mat/0604437
[13] Y. Léger L. Besombes, J. Fernández-Rossier, L. Maingault, H. Mariette. Phys. Rev. Lett**97**, 107401 (2006).
[14] D. L. Klein, R. Roth, A. K.L. Lim, A. P. Alivisatos, and P. L. McEuen Nature **389**, 699 (1997)
[15] J. Seufert, M. Rambach, G. Bacher, A. Forchel, T. Passow, D. Hommel, Appl. Phys. Lett. **82**, 3946 (2003)
[16] Yi Cui *et al.*, Nano Lett. **5**, 1519 (2005)
[17] T. Flissikowski, A. Hundt, M. Lowisch, M. Rabe, and F. Henneberger Phys. Rev. Lett. **86**, 3172-3175 (2001)
[18] L. Besombes, K. Kheng, L. Marsal, H. Mariette, Phys. Rev. B**65**, 121314 (2002)
[19] A. A. Maksimov et al. Phys. Rev. B**62**, R7767 (2000)
[20] J. Seufert *et al.*, Phys. Rev. Lett. **88** 027402, (2002)
[21] G. Bacher *et al.*, Phys. Rev. Lett. **89** , 127201 (2002)
[22] P. S. Dorozhkin et al., Phys. Rev. B **68**, 195313 (2003)
[23] S. Mackowski *et al.* Appl. Phys. Lett. **84**, 3337 (2004).
[24] S. C. Erwin *et al.*, Nature **436**, 91 (2005)
[25] J. Wunderlich *et al.* Phys. Rev. Lett**97**, 077201 (2006)
[26] H. Ohno *et al.*, Nature, **408**, 944 (2000)
[27] H. Boukari *et al.*, Phys. Rev. Lett. **88**, 207204 (2002).
[28] D.Chiba *et al.*, Science **301**, 943 (2003)
[29] J. I. Climente, M. Korkusinski, P. Hawrylak, and J. Planelles Phys. Rev. B **71**, 125321 (2005)

[30] F. Qu, P. Hawrylak, Phys. Rev. Lett. **95**, 217206 (2005)
[31] X. Huang, A. Makmal, J. R. Chelikowsky, and L. Kronik, Phys. Rev. Lett. **94**, 236801 (2005)
[32] A. O. Govorov, Phys. Rev. B**72** , 075359 (2005). A. O. Govorov, Phys. Rev. B**72** , 075358 (2005).
[33] A. K. Bhattacharjee and J. Pérez-Conde Phys. Rev. B**68**,045303 (2003)
[34] A. O. Govorov, Phys. Rev. B **70**, 035321 (2004) A. O. Govorov and A. V. Kalameitsev Phys. Rev. B **71**, 035338 (2005)
[35] A. Efros, E. Rashba, M. Rosen, Phys. Rev. Lett. **87**, 206601 (2001)
[36] F. V. Kyrychenko and J. Kossut, Phys. Rev. B**70** , 205317 (2004)
[37] J. Fernández-Rossier and L. J. Sham, Phys. Rev. B **64**, 235323 (2001)
[38] L. Brey, C. Tejedor and J. Fernández-Rossier Appl. Phys. Lett. **85**, 1996 (2004)
[39] A. K. Bhattacharjee and Phys. Rev. B**51**,9912 (1995)
[40] E. M. Chudnovsky and L. Gunther, Phys. Rev. Lett. **60**, 661 (1988) E. M. Chudnovsky, Phys. Rev. Lett**72**, 3433 (1994)
[41] J. Lambe and C. Kikuchi, Phys. Rev. **119**, 1256 (1960). D. Scalbert *et al.*, Solid State Communications **66**, 571 (1988).
[42] N. S. Norberg , D. R. Gamelin J. Phys. Chem. B**109**,20810 (2005)
[43] H. B. Heersche *et al.*, Phys. Rev. Lett. **96**, 206801 (2006)
[44] Moon-Ho Jo *et al.*, cond-mat/0603276